GEO India 2018

PaperID **AU347**

Author **JAYANTA DUTTA , Reliance Industries Limited , India**

Co-Authors **AJIT SAHOO , MUKUL SRIVASTAVA**

3D Pore Pressure Modelling of a Shale Gas Reservoir and its Implication

Authors

Jayanta Dutta[1], Ajit Sahoo[1], Mukul Srivastava[1]

[1]*Exploration, Reliance Industries Limited, Reliance Corporate Park, Navi Mumbai, India, 400701.*

Contact Person: Jayanta.dutta@ril.com, jeant_iitkgp@yahoo.co.in

Abstract

Study area is multi-fluid type shale gas reservoir with significant variations in reservoir top depth (9000 to 15000 feet) and thickness (100 to 500 feet). Such variations would significantly influence the pressure magnitude profile within the study area. Thus, 3D shale pore pressure model was planned to capture the pressure variations within the reservoir section across the field. Presence of secondary pressure generation mechanism (hydrocarbon generation, clay diagenesis) makes the estimation process further difficult. Therefore, a different strategy was adopted for 3D pore pressure modelling in this shale reservoir. To minimize the uncertainty on estimated pressure values due to use of multiple trend lines and also to handle the significant variations of reservoir geometry, single stratigraphy controlled normal compaction trend line was used to estimate the reservoir shale pore pressure.

1D and later 3D pore pressure volume was generated considering the co-exist scenario of both the pressure generation mechanism (disequilibrium compaction and secondary mechanism). Results suggest that the pore pressure profile & magnitude within the target shale reservoir is a combination effect of depth of reservoir occurrence, thickness and TOC (Total organic content). Increase in depth of occurrence and thickness along with high TOC (4 – 6%) has not only led to higher pressure from disequilibrium compaction process but also has prepared the favorable condition for secondary pressure generation mechanism (hydrocarbon generation, clay diagenesis) in the deeper part of the shale reservoir. These factors has resulted in additional high pressure (>1500- 2000 psi) than the regional pressure trend line in the deeper part with pressure contribution from secondary mechanism increases from shallower part (900 psi) to deeper part (1500 psi). Two different pressure regimes were inferred from 3D model – (i) shallower (<11500 psi), and (ii) deeper (>11500 psi). 3D pore pressure volume can be used for sweet spot identification through highlighting areas having high overpressure. Also, lateral pore pressure variations across the field would help in evaluating the hydro-frac job feasibility, procedure and optimization. As, the field is having two different pressure regimes, different completion strategy could be required for the shallower and deeper part respectively.

Introduction

Two game changer technology in shale gas industry are – horizontal pad drilling and multi-stage hydro-frac. Different sub-surface geomechanical parameters are found to effect these two prime factors- like pore pressure, stresses, rock mechanics, stress directions, natural fractures etc. Therefore, geomechanics has evolved as a strong tool to model these parameters accurately in order to enhance the shale gas production. The first task to build the geomechanical model for a shale gas reservoir is to estimate the pore pressure within the shale formation. Pore pressure has also been found to be directly linked in defining the magnitude of other geomechanical parameters like – horizontal stresses, fracture gradient, brittleness (**Dutta et al., 2017**), which makes it important to estimate the shale pressure accurately. However, direct pressure measurements cannot be done in low porosity (<10%) and permeability (micro to nano Darcy) bearing shale formation. Therefore, it demands a more vigilant understating on pressure generation mechanisms and thereafter the estimation method. Pore pressure generation mechanism can be categorized into two prime segment - Disequilibrium compaction related overpressure **(Osborne and Swarbrick, 1997)** and secondary pressure generation mechanism like hydrocarbon generation related fluid expansion, clay diagenesis, hybrid **(Bowers, 1994; Osborne and Swarbrick, 1997; Tingay et al., 2013).** Each mechanism is having different petrophysical signatures and, thus, requiring different pore pressure prediction strategies **(van Ruth et al., 2004; Tingay et al., 2009a).**

Study area is a multi-fluid type (oil, dry gas) bearing unconventional shale reservoir with significant variations in reservoir top depth (9000 to 15000 feet). Pore pressure plays a crucial role in shale gas production profile, which demand an in-depth analysis of pore pressure variation across the field. Knowledge of pore pressure variations across the field would not only helps in identifying sweet spots but also in optimization of hydro-frac job. 3D pore pressure modelling was performed in two stages – (1) 1D pore pressure analysis, (2) 3D pore pressure modelling.

1D Pore Pressure Modelling

Total 19 pilot wells were selected for 1D well level pore pressure analysis. First thing to do in pressure estimation is to know the pressure generation mechanism. Shale reservoir in this study area is having high TOC content (avg. 4- 6 %). The field is a multi-fluid type (oil to dry gas) reservoir, which suggest a likelihood additional pressure contribution due to fluid expansion (kerogen to hydrocarbon generation) process. Also, the TOC content shows increasing trend with depth **(Figure 1)** from shallower (4%) to deeper part (6%), which imply that the effect to be more prominent in the deeper part than the shallower part.

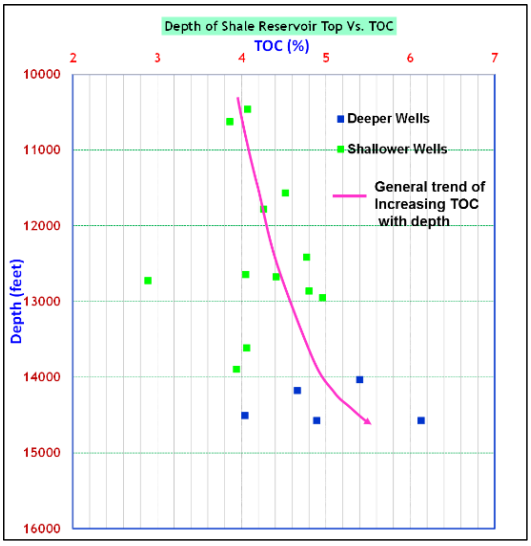

Figure 1. High TOC (4-6%) in the shale reservoir section suggest likelihood presence of fluid expansion related (kerogen to hydrocarbon generation) additional pressure contribution in this multi-fluid type reservoir.

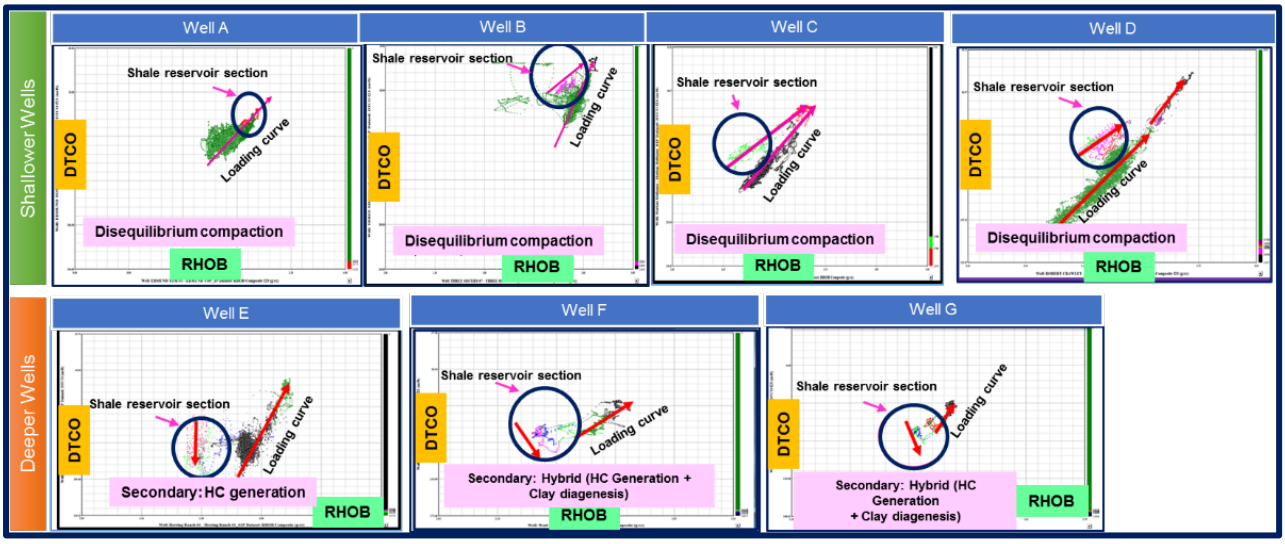

Figure 2. DTCO-RHOB crossplots shows prominent signatures of different secondary pressure generation mechanisms in deeper wells.

Sonic-density crossplot was used as a supportive tool to identify different pressure generation mechanism in this shale reservoir section. Sonic-density crossplots have been widely used as a method to identify the pore

pressure generation mechanism, specifically between primary or secondary mechanism and type of secondary mechanism – like fluid expansion, clay diagenesis, hybrid **(Hoesni, 2004; Tingay et al., 2013).** Selected pilot wells were broadly divided into two categories – (1) shallower wells (Reservoir top depth < 14000 ft), and deeper wells (Reservoir top depth >14000 ft). Sonic-density crossplots **(Figure 2)** of the shallower wells shows that the shale reservoir section is either following the disequilibrium compaction loading curve of the overburden shale section (i.e. increasing sonic and density with increase in pore pressure) or laying on this loading curve. Therefore, it suggest that the disequilibrium compaction is the only pressure generation mechanism in the shallower part. Whereas, sonic-density crossplots shows prominent signatures of secondary pressure generation mechanism in the deeper wells like, fluid expansion (TOC to gas generation - Well E) and hybrid mechanism (gas generation + clay diagenesis – Well F & G). Therefore, along with disequilibrium compaction related overpressure, deeper parts are likely to get extra pressure from secondary mechanism. Clay diagenesis signatures are seen in the mineralogy data of the deeper parts. DTCO-RHOB crossplots of deeper wells also shows that the log values are significantly lower than the overburden shale section **(Figure 2)**. This major shift in the values could be because of geological discontinuity between the reservoir and overburden section and/or relatively high amount of gas in the deeper wells which is effecting the logs (deeper wells are gas bearing, whereas shallower wells are oil/condensate bearing). However, the main criteria to identify the pressure generation mechanism is the overall trend of the DTCO-RHOB within the shale reservoir section. In this study area, based on this trend analysis, prominent indication of secondary mechanism in pore pressure generation has been identified in the deeper wells. The distinct shift in the petro-physical logs also directing to use of two different pressure prediction methods for overburden and shale reservoir respectively. DTCO-RHOB crossplots does not shows any secondary mechanism in shallower part, which might be because of maturity and mineralogy variations across the reservoir. In terms of maturity window, deeper wells comes in dry gas window. Whereas, shallower parts of the field is in the liquid (oil) to condensate window. So, the fluid expansion effect is likely to be more prominent in the deeper part. Also, the clay percentages are less in shallower part (<20%) and is gradually increasing in the deeper part, which is likely to effect petro-physical log signatures. Therefore, secondary mechanism can be more prominently seen in the deeper wells than shallower.

Estimation of shale pressure is difficult as there is no direct measurement of shale pressure, alike in sand formation. Most of the pore pressure estimation methods in shale formation are based on porosity-effective stress relationship and used for disequilibrium compaction related pressure estimation. But, secondary mechanism related overpressures are not associated with significant porosity anomaly and will not be correctly estimated from porosity-effective stress relationship **(Bowers, 1994; Tingay et al., 2009a).** So, a different strategy is required to estimate pressure in shale having secondary pressure contribution. Amongst different pore pressure method, **Eaton (1972)** method is commonly used to estimate shale pressure generated from disequilibrium compaction process. The Eaton (1972) method estimates pore pressure within the shale formation from the ratio of acoustic travel time expected in normally pressured formations versus the observed acoustic travel time. Below equation **(Equation 1)** is the Eaton (1972) method for pore pressure (P_p) estimation in shale.

$$P_p = \sigma_v - (\sigma_v - P_h)*(\Delta t_{norm} / \Delta t)^{x} \quad \text{.....Equation 1}$$

Where, P_h is the hydrostatic pore pressure, Δt_{norm} is the acoustic travel time from the normal compaction trend at the depth of investigation, σ_v is vertical stress, and Δt is the observed acoustic travel time from the sonic log, x is an exponent **(Eaton, 1972).** An Eaton exponent (x) of 3 is typically used and has been found to work well for formations where pore pressure are generated by disequilibrium compaction mechanism **(Eaton, 1972; van Ruth et al., 2004; Tingay et al., 2009a).** The absence of significant porosity anomaly requires a high Eaton exponent to amplify the typically smaller sonic velocity response associated with gas generation overpressure **(Tingay et al., 2013).** Along with disequilibrium compaction, to incorporate the contribution from secondary mechanism a different Eaton exponent value was used in the **equation 1.** Based on available information on pore pressure within the shale reservoir section of the area, Eaton exponent of 5 has been used in the **equation 1** to incorporate the extra pressure contributed from secondary mechanism.

Defining the normal compaction trend line (NCTL) for the shale reservoir formation in study area was challenging because of high lateral variation in reservoir top depth (~ 6000 feet) and involvement of secondary mechanism. Using multiple trend lines may led to uncertainties in pore pressure estimation. To overcome these challenges and minimize the uncertainties on pore pressure estimation, we have used single depth based stratigraphy controlled trend line within the shale reservoir section **(Figure 3)**. Also, based on distinct shift seen in DTCO-RHOB crossplots **(Figure 2),** a different single trend line has been used for the

overburden shale section. Basis of generating this stratigraphy controlled trend line was the available pore pressure database of the area and also the compaction trend of the shale just above the reservoir.

Five deeper wells at around 14000-15000 ft shows abnormally higher pressure (> 1500 - 2000 psi) than the regional pressure trend line **(Figure 4a),** due to additional pressure contribution from the secondary mechanism. It is also seen in the analysis that apart from depth of reservoir occurrence, the reservoir thickness is having noticeable effect on overpressure magnitude. Two wells having similar reservoir top depth from shallower part (Well K & J) and deeper part (Well F & H) respectively shows increasing trend in pore pressure with increase in reservoir thickness **(Figure 4b).** Additional pressure contribution from secondary mechanism is 900 -1000 psi in the shallower part. Whereas, contribution is higher (1500 psi) in the deeper parts **(Figure 4c)**. The 500 psi extra pressure contribution from secondary mechanism in deeper parts is due to relatively higher TOC and prominent secondary mechanisms (due to deeper depth and higher thickness). Deeper depth of reservoir occurrence, higher thickness along with high TOC has led to have higher pressure contribution from both primary and secondary pressure generation mechanisms in the deeper part than shallower. This dependency of pore pressure on different factors (depth, thickness, TOC) has led to significant lateral variations of pore pressure profile within the shale reservoir section and thus, 3D model is require to generate to capture the pressure variations across the field.

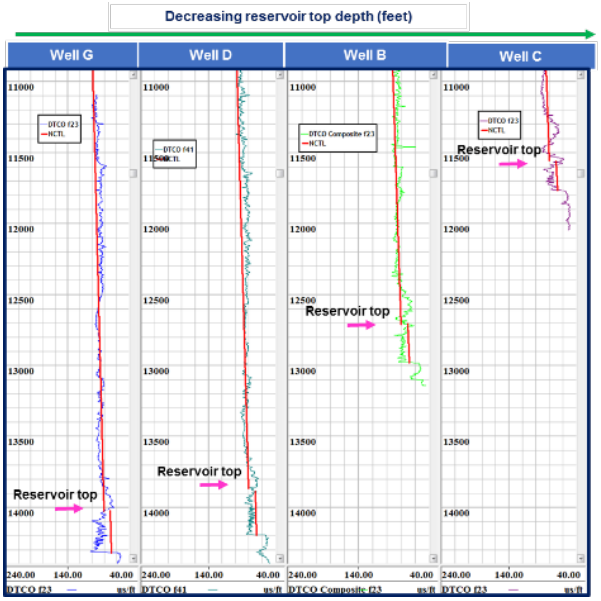

Figure 3. Separate trend line for overburden shale and reservoir shale respectively. Single depth based stratigraphy controlled trend line was used for the shale reservoir section.

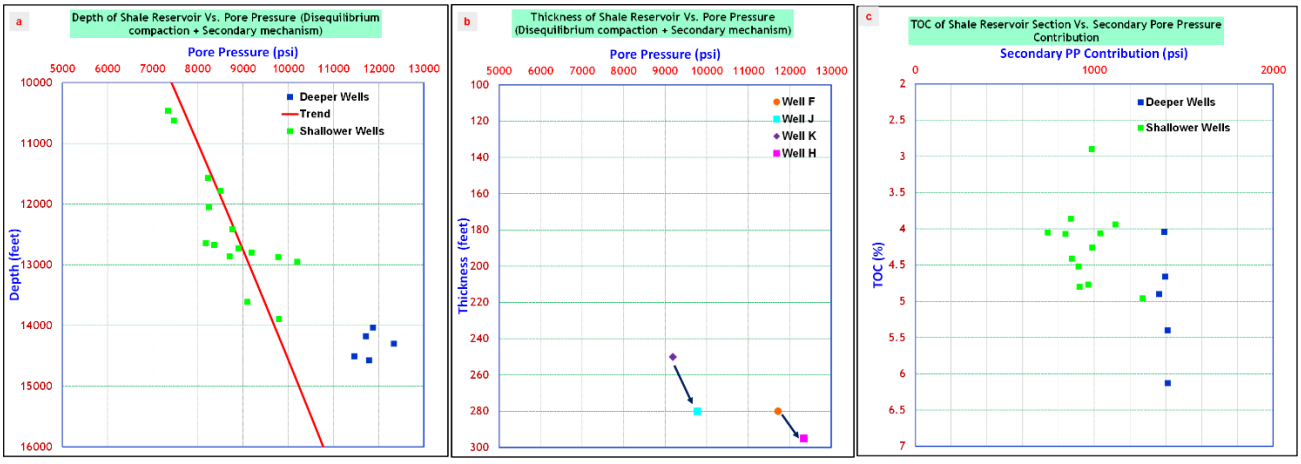

Figure 4. (a) Pore pressure in the deeper wells has deviated from the regional pressure trend of the field. **(b)** Increasing trend in pressure with increase in thickness can be seen between two wells having similar reservoir depth of occurrence. **(c)** Figure shows the additional pressure contribution from secondary mechanism apart from disequilibrium compaction.

3D Pore Pressure Modelling

Total 18 wells were used in building the 3D pore pressure model of the area. 3D seismic calibrated PSDM volume was used in 3D pore pressure modelling. 3D DTCO volume was generated from 3D seismic volume using CoKriging method with well DTCO. After multiple rigorous steps, 3D density cube was built with the help of generated 3D DTCO cube and well density data. Consequently, vertical stress was computed from build 3D density cube. NCTL trend of all the 18 wells were populated in 3D by Inverse distance weighting (IDW) method. Subsequently, two separate 3D NCTL volume were generated for overburden and reservoir section respectively. Then, a final single composite NCTL volume was developed to estimate pore pressure in this field. 3D pore pressure model has been build considering the co-exist scenario of secondary mechanism with primary disequilibrium compaction. Based on **Eaton (1972)** method, final 3D pore pressure volume was generated for the shale reservoir section with the inputs of 3D NCTL volume, DTCO volume, vertical stress volume, hydrostatic pressure volume and Eaton exponent of 5. Eaton exponent of 3 was used for the overburden shale section, which is having only disequilibrium compaction process related overpressure.

Discussion and Conclusion

A rigorous workflow was carried out to generate 3D pore pressure volume for the study area. **Figure 5a** shows the average pore pressure map of the shale reservoir section in the study area. Pressure magnitudes within the shale reservoir varies from 8000 to 13000 psi. Blue dotted line marked the high pressure line differentiating shallower part (<11500 psi) and deeper part (>11500 psi). In the shallower parts, maximum estimated pressure is ~11500 psi. Within this shallower part, noticeable pressure anomalies can be seen. These anomalies can be well explored and used in sweet spot identification. Deeper wells are having pressure in between 11500 – 13000 psi. **Figure5b** shows, how the pore pressure within the shale reservoir section is increasing from shallower to deeper section. Increase in the depth of reservoir occurrence (shallower to deeper) and thickness can also be seen in parallel with the increase in pore pressure.

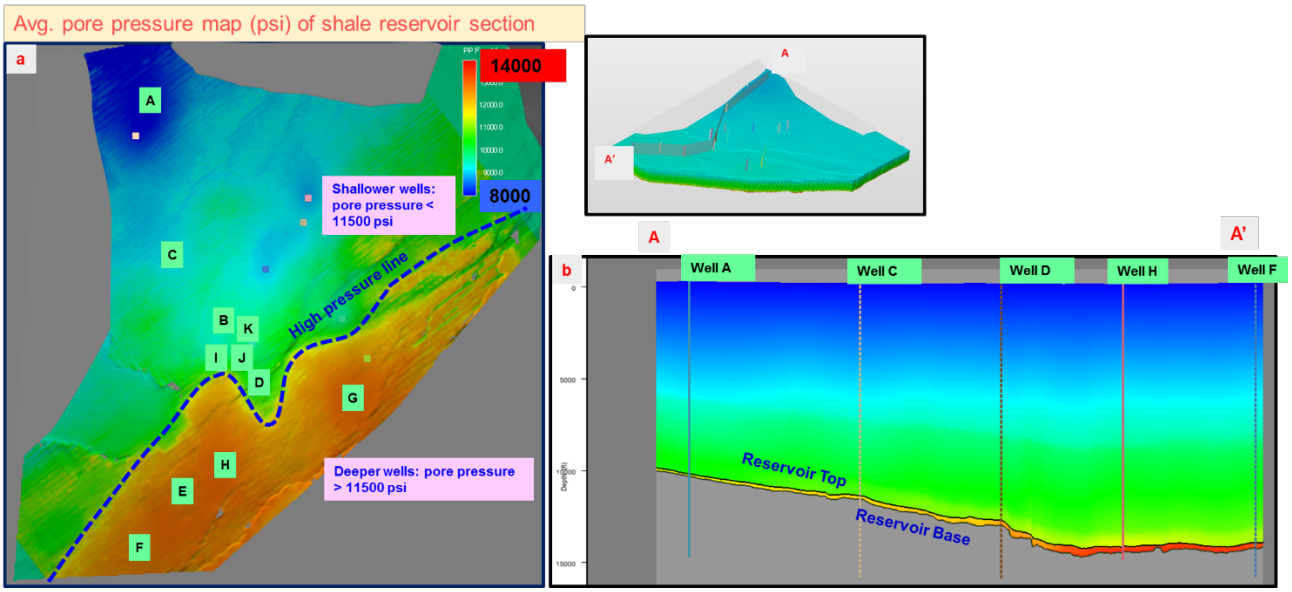

Figure 5. (a) Average pore pressure map of the shale reservoir section with high pressure line (dotted blue line) differentiating shallower part (pressure < 11500 psi) from deeper part (pressure >11500 psi), **(b)** Arbitrary cross section showing increase in pore pressure within shale reservoir from shallower to deeper part of the field. Depth of reservoir occurrence and thickness also shows increase from shallower to deeper part.

Figure 6a shows the increase of the reservoir top depth of the study area from 9000 feet to 15000 feet. This significant increase in reservoir occurrence depth has led to large variations in overburden sediment vis-à-vis vertical stress, which has caused large pressure variations across the field from shallower to deeper section. We have also marked the high pressure line to differentiate the deeper section having significant contribution from both primary and secondary pressure generation mechanism. Gross thickness map **(Figure 6b)** shows large variation of shale reservoir thickness from 100 to 500 feet. Gross thickness map **(Figure 6b)** shows significant increase of the shale reservoir thickness in the deeper section (below the marked high pressure line). This increase in depth of occurrence and thickness below the marked high pressure line has not only led

to higher pressure from disequilibrium compaction process but also has prepared the favorable condition for secondary mechanism (fluid expansion, clay diagenesis). Overpressure map (**Figure 6c)** is showing the effect of depth of occurrence, gross thickness, TOC and different pressure generation mechanism on pore pressure magnitude within the shale reservoir section of the study area. Overpressure map can be used to identify sweet spots through identifying areas having high pressure. Pressure magnitude values can be taken as an input in hydro-frac simulation study to understand the job feasibility and fracture behavior during HF job. Overpressure map (**Figure 6c)** clearly suggest two different pressure regimes (shallower and deeper) in the field. Pore pressure within the shale formation found to be closely linked with stresses magnitudes and rock mechanical properties of the rock. Therefore, same completion strategy may not work in two different pressure regimes and different completion strategy could be required. To further validate it, more detailed geomechanical analysis (stress, rock mechanics, brittleness) is recommended to be carried out.

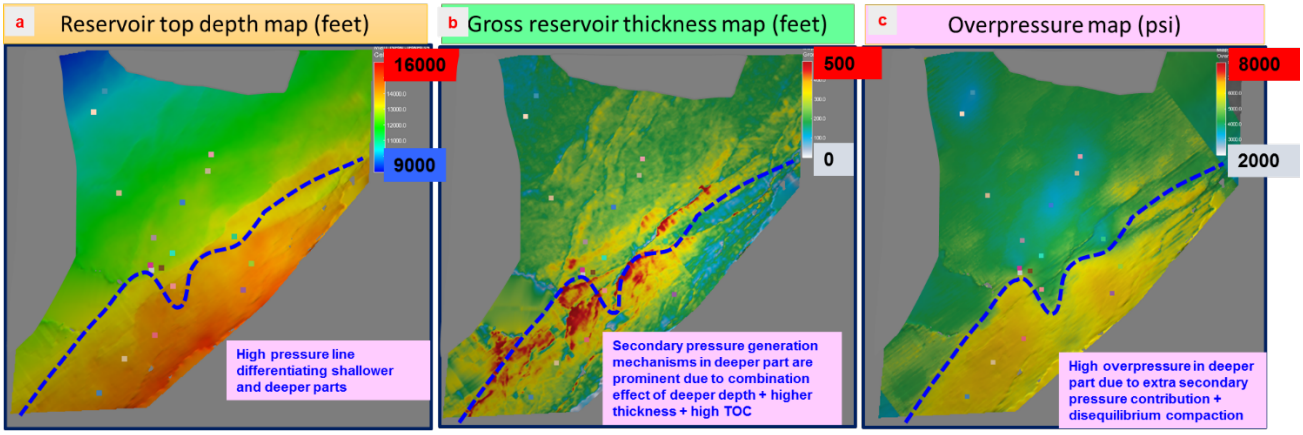

Figure 6. (a) Reservoir top depth map showing the large variation of reservoir top depth across the field, **(b)** Gross thickness map shows the higher thickness in the deeper section below the high pressure line, **(c)** Overpressure map showing the lateral variation of pressure which can be used for sweet spot identification and hydro-frac job optimization. Figure also shows two prominent pressure regimes (shallower and deeper) in the field.

Acknowledgements:

We thank and appreciate the critical feedbacks/suggestions received from the reviewer that helped us to improve the contents of the paper. We thank and appreciate the critical inputs received from Neeraj Sinha, Suraj P. Sharma, Nitin Bhardwaj, Ashutosh Kumar, Deepika Saini which helped us to improve the overall process and contents of the paper. We would like to thanks Reliance Industries Ltd., (E & P) Petroleum Business for giving us the permission to publish this paper.

References:

Bowers, G. L., 1994, Pore pressure estimation from velocity data: Accounting for overpressure mechanisms besides undercompaction: 1994 International Association of Drilling Contractors/Society of Petroleum Engineers Drilling Conference, p. 515–530.

Dutta, J., Bhardwaj, N. and Kumar, A., 2018. Integration of mini-frac stress results with core data to identify ductile behavior of overpressured sandstone reservoir in deep-water offshore Krishna-Godavari basin, India. Geomechanics and Geophysics for Geo-Energy and Geo-Resources, 4(1), pp.11-28.

Eaton, B. A., 1972, Graphical method predicts geopressures worldwide: World Oil, v. 182, p. 51–56.

Hoesni, J., 2004, Origins of overpressure in the Malay Basin and its influence on petroleum systems: PhD thesis, University of Durham, Durham, United Kingdom, 268 p.

Osborne, M. J., and R. E. Swarbrick, 1997, Mechanisms for generating overpressure in sedimentary basins: A reevaluation: AAPG Bulletin, v. 81, p. 1023–1041.

Tingay, M. R. P., R. R. Hillis, R. E. Swarbrick, C. K. Morley, and A. R. Damit, 2009a, Origin of overpressure and pore pressure prediction in the Baram Delta Province, Brunei: AAPG Bulletin, v. 93, p. 51–74, doi:10.1306/08080808016.

Tingay, M.R., Morley, C.K., Laird, A., Limpornpipat, O., Krisadasima, K., Pabchanda, S. and Macintyre, H.R., 2013. Evidence for overpressure generation by kerogen-to-gas maturation in the northern Malay Basin. AAPG bulletin, 97(4), pp.639-672.

van Ruth, P., R. R. Hillis, R. E. Swarbrick, and P. Tingate, 2004, The origin of overpressure in the Carnarvon Basin, Western Australia: Implications for pore pressure prediction: Petroleum Geoscience, v. 10, p. 247–257, doi:10.1144/1354-079302-562.